Enhancing the antimicrobial potential of lanthipeptides by employing different engineering strategies

Zhao, Xinghong

DOI:
10.33612/diss.127409437

Chapter 5

Silver@nisin nanoclusters are highly effective against biofilm-forming pathogens found in wound infection

Xinghong Zhao, Oscar P. Kuipers *

Department of Molecular Genetics, Groningen Biomolecular Sciences and Biotechnology Institute, University of Groningen, Groningen, 9747 AG, The Netherlands.

* Correspondence: o.p.kuipers@rug.nl (Oscar P. Kuipers)

In preparation.

Abstract

Wound infection is a serious threat to patients, in particular septic wound infections, which result in high mortality rates. Moreover, the treatment of wound infections with antimicrobial-resistant and/or biofilm-forming pathogens can be challenging. Nisin, a potent antimicrobial against Gram-positive pathogens, has been used in the food industry for decades. Silver has been approved by FDA as a topical antimicrobial. However, both nisin and silver as stand-alone therapy show insufficient anti-biofilm activity against bacterial pathogens. Here, we show that silver@nisin nanoclusters, with an average diameter of 60 nm, can be synthesized by microwave-assisted molecular self-assembly. The synthesized Ag@nisin NC showed higher antimicrobial activity than either silver nitrate or nisin alone. Notably, Ag@nisin NC showed potent anti-biofilm activity against *S. aureus*, *P. aeruginosa*, *A. baumannii*, *K. pneumoniae*, and *E. coli*, which are pathogens responsible for wound infections. Moreover, due to the nisin peridium, Ag@nisin NC showed much lower cytotoxicity than silver nitrate to a human kidney epithelium cell line. This work shows that microwave-assisted molecular self-assembly is a powerful and novel strategy to synthesize metal@antimicrobial peptide nanocomposites for biofilm-infected wound control.

Introduction

The skin plays a critical role in keeping microorganisms away from the underlying tissues of the human body. Wound infection caused by mechanical disruption of the skin or by burn is a serious threat to patients [1]. Particularly, septic wound infections can result in high mortality rates [2]. Previous studies demonstrated that *Staphylococcus aureus*, *Pseudomonas aeruginosa*, *Acinetobacter baumannii*, *Klebsiella pneumoniae*, and *Escherichia coli* are major contributors to wound infections [1–6]. Moreover, antimicrobial-resistant pathogens, including multi-drug resistant *P. aeruginosa* (MDR PA), *A. baumannii* (MDR AB) and methicillin-resistant *S. aureus* (MRSA), are playing an important role in the high morbidity and mortality rate of wound infections [4]. Even more seriously, these major contributors (*S. aureus*, *P. aeruginosa*, *A. baumannii*, *K. pneumoniae*, and *E. coli*) usually form biofilms in the infected wound, and these biofilms make wound infections more difficult to treat [6]. Therefore, new strategies are required to treat wound infections.

Nanotechnology-based antimicrobials have been proposed as a promising source of antimicrobial agents, which can penetrate biofilms and kill pathogens including multidrug-resistant strains [7]. Silver-based nanocomposites showed potent antimicrobial activity against both planktonic pathogens and pathogen biofilms [8]; moreover, they showed strong synergistic effects with antibiotics [9–11]. Ag is a widely used material for producing metal-based nanocomposites, and it is currently approved by the U.S. Food and Drug Administration (FDA) as a topical antimicrobial [12]. Nisin is a natural antimicrobial peptide produced by various *Lactococcus lactis* strains, and it has been approved and used in the food industry for decades over the world [13,14]. More recently, the antimicrobial effects of nisin against mastitis, respiratory-, gastrointestinal- and skin infections have been investigated, and the results showed that nisin had potent antimicrobial effect against Gram-positive caused infections [15]. Therefore, Ag- and nisin-based nanocomposites may show potent antimicrobial activity against both planktonic pathogens and pathogen biofilms in wound infections.

In this study, we introduce a simple, ultrafast and quality-stable method to construct Ag@nisin nanoclusters by employing a strategy of microwave-assisted molecular self-assembly. Under the selected conditions, Ag@nisin NC

with an average diameter of 60 nm was obtained. Notably, the synthesized Ag@nisin NC showed potent antimicrobial activity and anti-biofilm activity against *S. aureus*, *P. aeruginosa*, *A. baumannii*, *K. pneumoniae*, and *E. coli*, which are pathogens responsible for wound infections. Moreover, due to the nisin peridium, Ag@nisin NC showed much lower cytotoxicity than $AgNO_3$ to a human kidney epithelium cell line. This work shows that microwave-assisted molecular self-assembly is a powerful and novel strategy to synthesize metal@antimicrobial peptide nanocomposites for wound biofilm-infection control.

Results

Synthesis and characterization of Ag@nisin NC. The synthesis of Ag@nisin NC was performed at different concentrations of nisin and different microwave irradiation times, and the size of the products was determined by dynamic light scattering (DLS). Ag@nisin NC was obtained with the smallest average size under the condition of addition 4 mL of 4 mM $AgNO_3$ solution to 95 mL of nisin at a concentration of 62.5 µM and microwave irradiation for 15 s at 700 W (data not shown). A SEM assay was used to investigate the morphology of Ag@nisin NC, and the results show that Ag@nisin NC with an irregular morphology was obtained (Fig. 1a). Moreover, the size distribution of synthesized Ag@nisin NC, by counting 300 particles of SEM, is shown in Fig. 1b, and the results show that Ag@nisin NC with an average size of 60±19 nm was obtained. After that, X-ray diffraction (XRD) was used to investigate the phase of the Ag@nisin NC. As shown in Fig. 1c, the diffraction features appearing at 32.3°, 46.2°, 67.5° and 76.7° are corresponding to the (111), (200), (220) and (311) planes of the cubic phase of Ag, respectively [16,17]. These results indicate that silver crystals were formed in the Ag@nisin NC. Furthermore, to verify whether the nanocluster was formed by nisin and a silver crystal, an attenuated total reflection infrared (ATR-FTIR) assay was performed. The characteristic peaks of nisin at 1658.45 and 1527.32 are corresponding to a C=O stretching of amide I and N-H bending of amide II, respectively (Fig. 1d) [18–20]. The same peaks were also observed for the Ag@nisin NC (Fig. 1d). These results confirmed that the synthesized Ag@nisin NC consists of silver crystal and nisin.

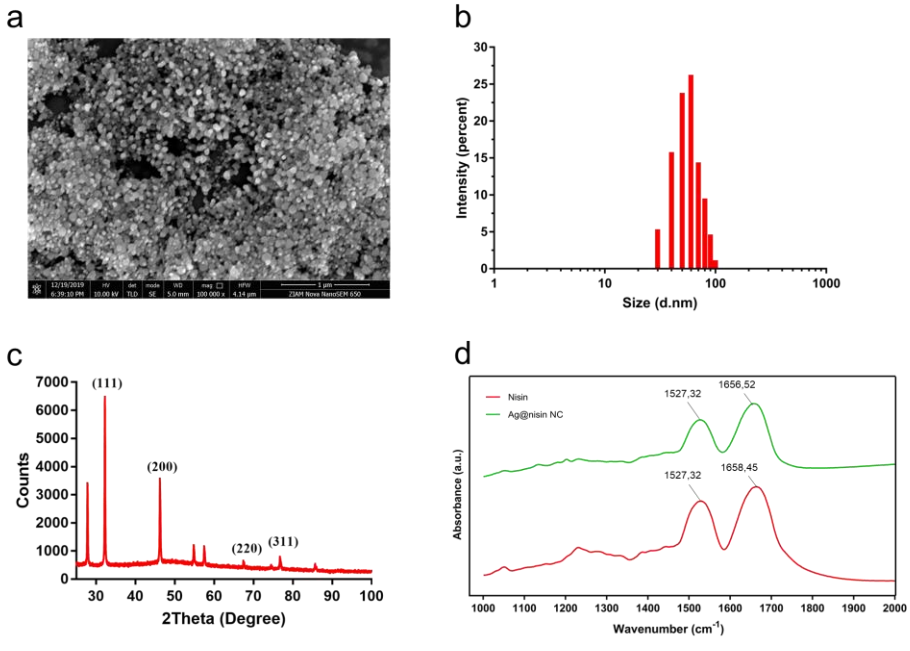

Figure 1 a, SEM of Ag@nisin NC; **b**, size distribution of synthesized Ag@nisin NC by counting 300 particles of SEM result (average size 60 nm); **c**, XRD of Ag@nisin NC; **d**, FTIR of Ag@nisin NC and nisin.

Ag@nisin NC exerts potent antimicrobial activity against biofilm-forming pathogens of wound infection. To determine the antimicrobial activity of Ag@nisin NC, a MIC assay was performed. $AgNO_3$ and nisin were used as controls. Nisin showed potent antimicrobial activity against *S. aureus* (LMG15975, MRSA), which is a Gram-positive bacterium (Table 1). However, nisin showed very weak antimicrobial activity against most of the tested Gram-negative bacteria pathogens (Table 1). These results are consistent with previous studies [21,22]. $AgNO_3$ showed potent antimicrobial activity against all of the tested strains (Table 1). Moreover, it was shown to have a better antimicrobial activity against Gram-negative bacteria than Gram-positive bacteria (Table 1). Ag@nisin NC showed potent antimicrobial activity against all of the tested pathogens, and it showed 2-fold better antimicrobial activity against all tested Gram-negative bacteria than $AgNO_3$ (Table 1). Importently, Ag@nisin NC showed 4-fold better antimicrobial activity against tested Gram-positive bacteria than $AgNO_3$, which might be caused by the nisin lipid II

binding site helping the Ag@nisin NC to be more specifically targeting Gram-positive bacteria. Moreover, Ag@nisin NC showed much better antimicrobial activity against tested Gram-negative bacteria than nisin (Table 1).

Table 1 Antimicrobial activity of Ag@nisin NC against pathogenic microorganisms of wound infection.

Organism and genotype	MIC (μg/mL)		
	Nisin	$AgNO_3$	Ag@nisin NC
A. baumannii LMG01041	16	2	1
P. aeruginosa LMG 6395	128	4	2
E. coli LMG8223	64	4	2
K. pneumoniae LMG20218	128	8	4
S. aureus LMG15975 (MRSA)	4	16	4

The MIC was determined by broth microdilution. MRSA, methicillin-resistant S. aureus.

Ag@nisin NC showed low cytotoxicity to a human kidney epithelium cell line. To assess the safety of Ag@nisin NC to human beings in an initial test, the cytotoxicity of antimicrobials to a human kidney epithelium cell line was evaluated by an XTT assay. Human kidney epithelium cells were incubated in the presence of different concentrations of antimicrobials. After 24 h incubation, the cell viability was determined by using a XTT kit. Under the experimental conditions used, human kidney epithelium cells were unaffected by the presence of nisin at 128 μg/mL (Fig. 2). $AgNO_3$ showed potent cytotoxicity to a human kidney epithelium cell line at 4 μg/mL (Fig. 2), which is lower than most of the tested MIC values (Fig. 2, Table 1). These results indicate that $AgNO_3$ is not suitable as an antimicrobial agent when used alone. Therefore, we did not use $AgNO_3$ any more in further studies. However, Ag@nisin NC did not show cytotoxicity to a human kidney epithelium cell line at concentrations of 8×MIC value against *A. baumannii* (LMG01041), 4×MIC against *P. aeruginosa* (LMG 6395) and *E. coli* (LMG8223), and 2×MIC against *K. pneumoniae* (LMG20218) and *S. aureus* (LMG15975, MRSA) (Fig. 2, Table 1). These results indicate that Ag@nisin NC is a high efficiency and low toxicity

antimicrobial agent.

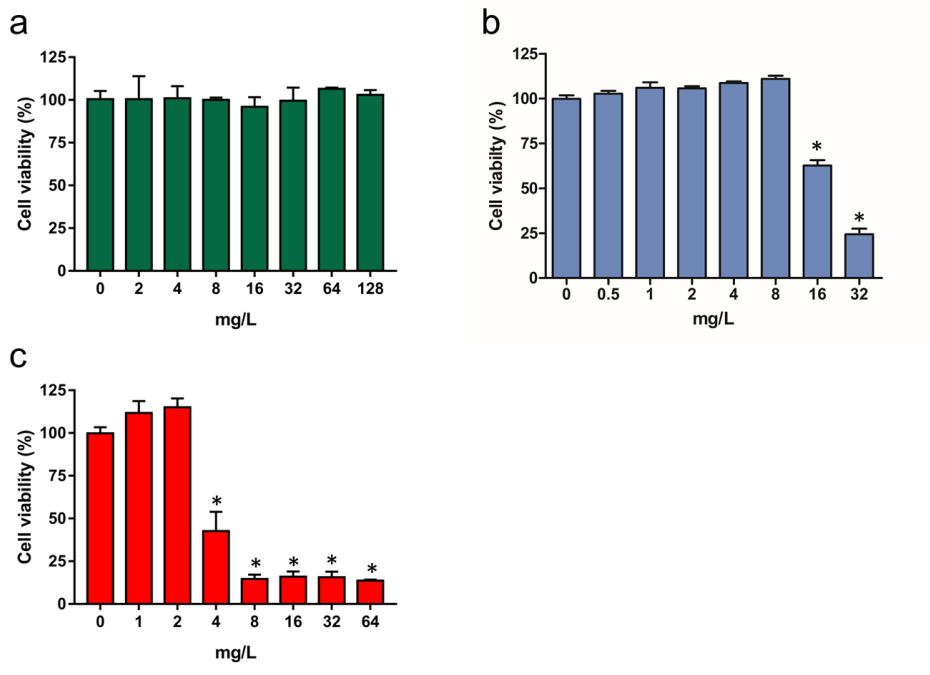

Figure 2 Percentage of cell viability of human kidney epithelium cell line after 24 h treatment with different concentrations of nisin, Ag@nisin NC and $AgNO_3$, respectively. **a**, nisin; **b**, Ag@nisin NC; **c**, $AgNO_3$. Data are representative of three independent experiments; the statistical significance of differences was performed by Pearson r2, ns: $p > 0.05$, *$p < 0.01$ vs. untreated cells.

Time-dependent killing of Planktonic pathogens by Ag@nisin NC. Measuring the time-dependence of antibiotic action is commonly used to establish whether a compound is bacteriostatic or bactericidal [23,24]. In this study, we monitored the killing kinetics of *A. baumannii* (LMG01041), *P. aeruginosa* (LMG 6395), *E. coli* (LMG8223), *K. pneumoniae* (LMG20218) and *S. aureus* (LMG15975, MRSA) cells exposed to either the synthesized Ag@nisin NC or nisin. Due to its pore-formation ability in the target cell membrane, together with cell wall biosynthesis inhibition, nisin is well known as a bactericidal lantibiotic [25]. The time-dependent killing results show that nisin killed all of the *A. baumannii* (LMG01041), *E. coli* (LMG8223) and *S. aureus* (LMG15975, MRSA) in 2 hours (Fig. 3 a, c and e). Moreover, nisin killed most of the *P. aeruginosa* (LMG 6395) and *K. pneumoniae* (LMG20218) in 8 hours (Fig. 3 b and d). However, nisin did not completely kill *P. aeruginosa* (LMG 6395) and *K. pneumoniae* (LMG20218) at 24 h after treatment (Fig. 3 b and d), and the

bacteria were grown to an OD_{600} of around 6 at 72 h after treatment. These results indicate that *P. aeruginosa* (LMG 6395) and *K. pneumoniae* (LMG20218) can easily get resistant against nisin even at a concentration of 256 µg/mL. Ag@nisin NC showed fast kill kinetics against all of the tested pathogens, which killed all of the *E. coli* (LMG8223), *K. pneumoniae* (LMG20218) and *S. aureus* (LMG15975, MRSA) in 1 h after treatment (Fig 3 c, d, and e), killed all of the *A. baumannii* (LMG01041) in 2 h after treatment (Fig 3 a) and killed all of the *P. aeruginosa* (LMG 6395) in 4 h after treatment (Fig 3 b).

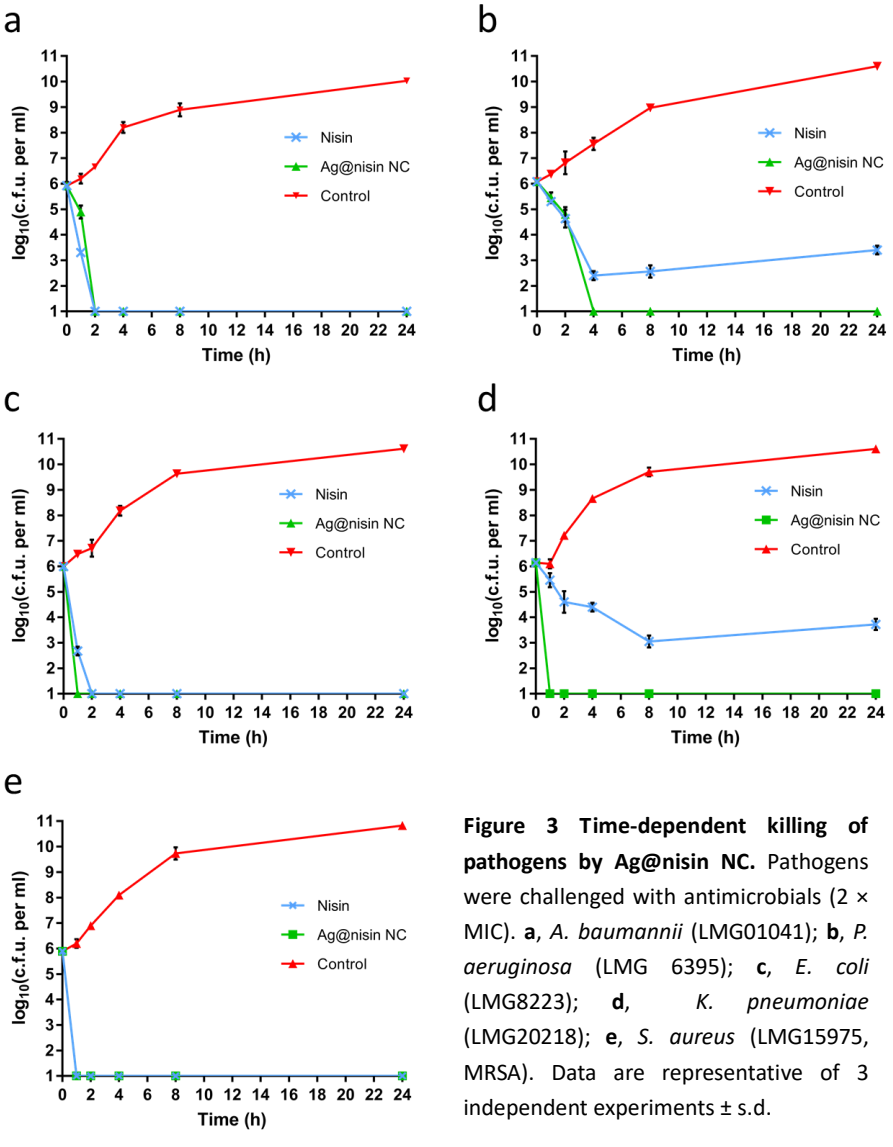

Figure 3 Time-dependent killing of pathogens by Ag@nisin NC. Pathogens were challenged with antimicrobials (2 × MIC). **a**, *A. baumannii* (LMG01041); **b**, *P. aeruginosa* (LMG 6395); **c**, *E. coli* (LMG8223); **d**, *K. pneumoniae* (LMG20218); **e**, *S. aureus* (LMG15975, MRSA). Data are representative of 3 independent experiments ± s.d.

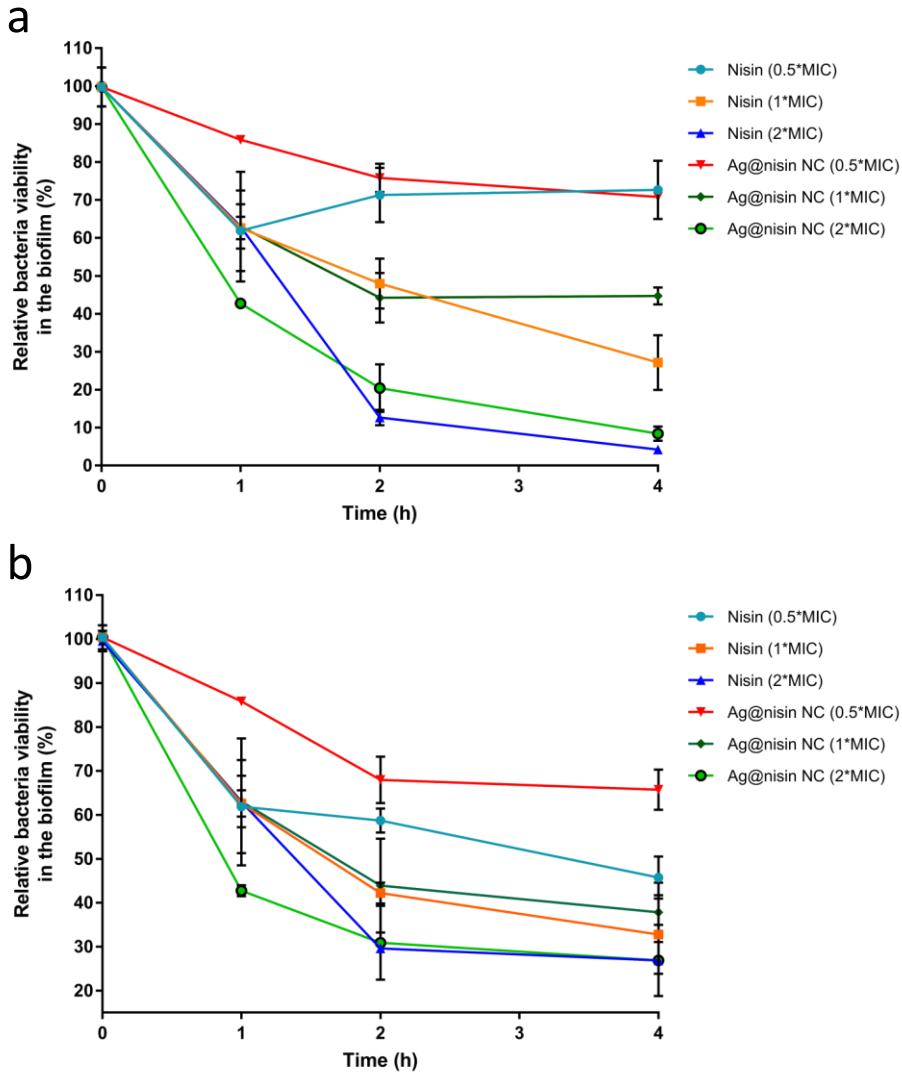

Figure 4 Anti-biofilm activity of Ag@nisin NC. a, Time–kill curves for *S. aureus* (LMG15975, MRSA) biofilm after treatment with antimicrobial agents; b, Time–kill curves for *A. baumannii* (LMG01041) biofilm after treatment with antimicrobial agents.

Ag@nisin NC showed potent anti-biofilm activity. An XTT assay was used to measure the anti-biofilm activity of antimicrobial agents in previous studies [26–28]. In this study, we used XTT assay to investigate the anti-biofilm activity of Ag@nisin NC. Ag@nisin NC showed the rapid killing of bacteria in a biofilm (Fig. 4 a, b). After 4 h of treatment, the viability of bacteria in a biofilm was only

26.8% for *A. baumannii* (LMG01041) and 8.4% for *S. aureus* (LMG15975, MRSA) under a 2×MIC treatment. Most of the killing happens in the first 2 hours after treatment, and a higher concentration of Ag@nisin NC showed better anti-biofilm activity. Furthermore, Ag@nisin NC significantly decreased bacterial viability in *P. aeruginosa* (LMG 6395), *E. coli* (LMG8223) and *K. pneumoniae* (LMG20218) biofilms after 4 h treatment (Fig. 5). Under a 2×MIC treatment, Ag@nisin NC killed 88.3% of *P. aeruginosa* (LMG 6395), 82.5% of *E. coli* (LMG8223) and 73.6% of *K. pneumoniae* (LMG20218) in their biofilms, respectively.

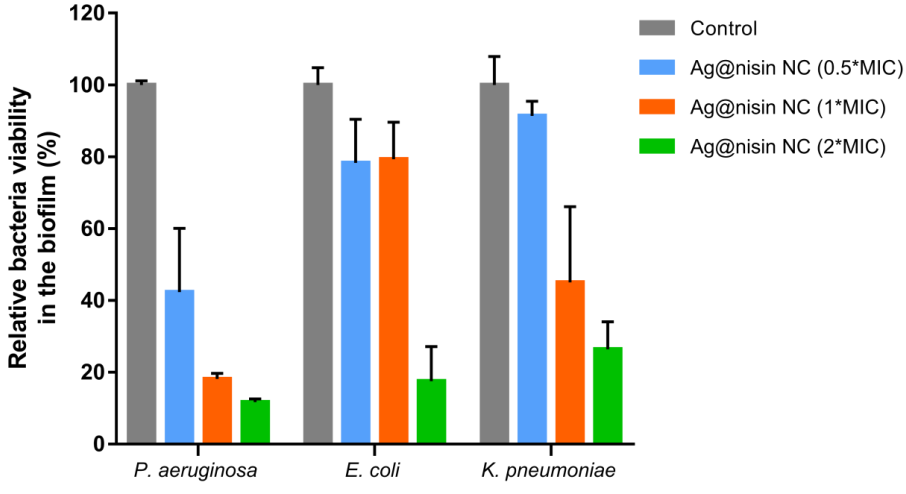

Figure 5 Anti-biofilm activity of different concentrations of Ag@nisin NC against *P. aeruginosa* (LMG 6395), *E. coli* (LMG8223) and *K. pneumoniae* (LMG20218) biofilms.

Discussion

Wound infection is a serious threat to patients, in particular septic wound infections, which result in high mortality rates [1,4]. Here we show a simple, ultrafast, and quality-stable method for Ag@nisin NC synthesis. The synthesized Ag@nisin NC showed potent antimicrobial and anti-biofilm activity against *A. baumannii*, *P. aeruginosa*, *E. coli*, *K. pneumoniae* and *S. aureus*, which are vital pathogens of wound infections.

Many methods have been used to construct silver nanocomposites, including

chemical, physical and biological methods [29]. Microwave-assisted synthesis of silver nanocomposites has many advantages, such as smaller size, narrower size distributions, shorter reaction times, reduced energy consumption, and better product yields etc. [30,31]. In this study, microwave-assisted synthesis of Ag@nisin NC was performed. The results showed Ag@nisin NC with an average size of 60 nm (diameter) was obtained, and it only needs 15 s to construct this narrower size distribution Ag@nisin NC. In contrast, previous studies showed that nisin@silver nanoparticles can be synthesized by incubation of silver nitrate and nisin at room temperature for 24 h [32], and the synthesized nisin@silver nanoparticles showed a 233 nm (diameter) average size [32], which is known to be without anti-biofilm activity [7]. These results demonstrate that microwave-assisted synthesis of Ag@antimicrobial peptide nanocomposites is a much more effective approach.

Most of clinical wound infections are mixed Gram-negative and Gram-positive pathogens infections [1–6]. Nisin has only potent antimicrobial activity against Gram-positive pathogens [21,22], which limited the application of nisin as an alternative control for wound infection. Silver has a potent bactericidal effect against both Gram-positive and Gram-negative pathogens [12,33], but it's difficult to balance antimicrobial activity with cytotoxicity. In this study, the synthesized Ag@nisin NC showed higher antimicrobial activity against both Gram-positive and Gram-negative pathogens than either nisin or $AgNO_3$ alone. Notably, Ag@nisin NC showed much lower cytotoxicity against mammalian cells than $AgNO_3$ alone. In contrast, antimicrobial peptide LL37 coated LL37@AgNP decreased the antimicrobial activity of $AgNO_3$ against tested Gram-negative pathogens [34]. These results indicate that a lanthionine-stabilized antimicrobial peptide nisin is more suitable to be used to synthesize silver nanocomposites. The stronger antimicrobial activity and lower cytotoxicity make Ag@nisin NC an attractive option to control wound infections.

Many of the isolates of clinical wound infections are biofilm producing strains [6].In this study, the synthesized Ag@nisin NC showed a broad-spectrum of anti-biofilm activity against both Gram-positive and Gram-negative pathogens found in wound infections (Fig. 4). These results are consistent with previous studies, which showed that silver nanoparticles have anti-biofilm activity [34–37].

In addition, silver nanocomposites show strong synergistic effects with antibiotics [9–11]. It could be also a good strategy to use Ag@nisin NC with other antibiotics for wound infections control.

In conclusion, a microwave-assistant ultra-fast method was performed to synthesize of Ag@nisin NC. The synthesized Ag@nisin NC showed potent antimicrobial and anti-biofilm activities against both Gram-negative and Gram-positive bacterial pathogens, which is 2-4 times better than clinically used ionic silver. Notably, the synthesized Ag@nisin NC showed much lower cytotoxicity than clinically used ionic silver against a human kidney epithelium cell line. These results suggest that Ag@nisin NC offer good application possibilities to treat wound infections.

Materials and methods

Assembly of Silver@nisin Nanocomposite. Nisin (99% purity, Handary S.A., Belgium) was dissolved in water (with an electronic resistance of 18.2 MΩ*cm, MQ) to concentrations of 125, 62.5 and 31.3 μM, respectively. Then 4 mL of 4 mM $AgNO_3$ (Sigma) was dropped into 95 mL of nisin solution at room temperature. Under microwave irradiation at power intensity of 700 W, the reaction of the mixture was carried out for 15, 30 and 60 S, respectively. After centrifugation at 10,000 × g for 15 min, the product was washed with MQ water three times.

Characterization of Ag@nisin NC. Dynamic light scattering (DLS, Malvern Panalytical) was used to determine the size of Ag@nisin NC in MQ water. A SEM was used to investigate the morphologies of the products. Attenuated total reflection infrared (ATR-FTIR) and X-ray diffraction (XRD) were used to investigate the composition and structure of Ag@nisin NC.

Minimum inhibitory concentration (MIC). MIC values were determined by broth micro-dilution according to the standard guidelines [38], and *A. baumannii* (LMG01041), *P. aeruginosa* (LMG 6395), *E. coli* (LMG8223), *K. pneumoniae* (LMG20218) and *S. aureus* (LMG15975, MRSA)) were used as indicator strains. Briefly, the test medium was cation-adjusted Mueller-Hinton broth (MHB). Cell concentration was adjusted to approximately 5×10^5 cells per ml. After 24 h of incubation at 37 °C, the MIC was defined as the lowest concentration of

antibiotic with no visible growth. Experiments were performed with biological replicates.

Cell Culture. The human kidney epithelium cells was maintained in complete DMEM supplemented with 10% (v/v) foetal bovine serum (FBS, Gibco), 100 U/mL penicillin (HyClone), and 100 µg/mL streptomycin (HyClone). For the maintenance medium (MM), the serum concentration was reduced to 2%. Cells were incubated at 37 °C with 5% CO_2 [39].

Mammalian cell metabolically active assay. The effect of materials to mammalian cell metabolically active was evaluated on human kidney epithelium cells by using the XTT (Cell Proliferation Kit XTT, AppliChem) assay. Briefly, cells in 96-well plates were exposed to different concentrations of materials in sextuplet. The test samples were suspended in MM (100 µL per well). After 24 h incubation, the XTT reagent was added to the cultures according to the manufacturer's instructions, and the plates were incubated at 37 °C for 2 h with 5% CO_2. Then, the absorbance values were measured by using a Varioskan™ LUX multimode microplate reader (Thermo Fisher Scientific) at 485 nm (reference 690 nm).

Planktonic time-dependent killing assay. This assay was performed according to a previously described procedure [24]. An overnight culture of cells (*A. baumannii* (LMG01041), *P. aeruginosa* (LMG 6395), *E. coli* (LMG8223), *K. pneumoniae* (LMG20218) and *S. aureus* (LMG15975, MRSA)) was diluted 50-fold in MHB and incubated at 37 °C with aeration at 220 r.p.m.. Bacteria were grown to an OD of 0.5, and then the cells concentration was adjusted to ≈1×10^6 cells per ml. Bacteria were then challenged with nisin (2*MIC) or Ag@nisin NC (2*MIC) in culture tubes at 37 °C and 220 r.p.m. Non-treated bacteria were used as negative control. At desired time points, one hundred 200 µL aliquots were taken, centrifuged at 8,000 g for 2 min and resuspended in 200 µL of MHB. Ten-fold serially diluted samples were plated on MHA plates. After incubated at 37 °C overnight, colonies were counted and c.f.u. per mL was calculated. Each experiment was performed in triplicate.

Anti-biofilm assay. The strains (*A. baumannii* (LMG01041), *P. aeruginosa* (LMG 6395), *E. coli* (LMG8223), *K. pneumoniae* (LMG20218) and *S. aureus*

(LMG15975, MRSA) were cultured for one day at 37 ℃ in 4 mL of tryptone soya broth (TSB, Oxoid). The cultures were diluted to at an OD_{600} of 0.01 in TSB, and 200 µL of the resulting bacterial suspension was aliquoted into the wells of a 96-well tissue culture-treated polystyrene plate (corning). After 24 h of growth at 37 ℃, the plates were washed thoroughly three times with PBS to remove unattached bacteria. Next, MHB containing 0, 0.5, 1 and 2 times MIC of nisin or Ag@nisin NC was added to the wells. The plates were incubated at 37 ℃ under shaking at 60 r.p.m.. XTT assay was used to assess the cell metabolically viability at 1, 2 and 4 h post exposure to the tested compounds (*A. baumannii* (LMG01041) and *S. aureus* (LMG15975, MRSA)) or 4 h post exposure to the tested compounds (*P. aeruginosa* (LMG 6395), *E. coli* (LMG8223), *K. pneumoniae* (LMG20218)). Briefly, after having removed the compounds, the plates were washed vigorously three times with PBS. After that, PBS (200 µL) containing 50 µL XTT (Cell Proliferation Kit XTT, AppliChem) was added to the wells and incubated at 37 ℃ for 2 h. The plates were then determined using a Varioskan™ LUX multimode microplate reader (Thermo Fisher Scientific) at 485 nm (reference 690 nm). Higher OD values correlated to higher numbers of viable pathogens in the biofilm. Each experiment was performed in triplicate.

Acknowledgments

X. Zhao was financially supported by the Chinese Scholarship Council (CSC). We thank Dr. Gert N. Moll (Lanthio Pharma, Rozenburglaan 13 B, Groningen, 9727 DL, Netherlands) for reading and improving the manuscript.

References

1. Vaez, H. & Beigi, F. Antibiotic susceptibility patterns of aerobic bacterial strains isolated from patients with burn wound infections. *Germs* **6**, 34 (2016).
2. Pallavali, R. R., Degati, V. L., Lomada, D., Reddy, M. C. & Durbaka, V. R. P. Isolation and in vitro evaluation of bacteriophages against MDR-bacterial isolates from septic wound infections. *PLoS One* **12**, e0179245 (2017).
3. Bessa, L. J., Fazii, P., Di Giulio, M. & Cellini, L. Bacterial isolates from infected wounds and their antibiotic susceptibility pattern: some remarks about wound infection. *Int. Wound J.* **12**, 47–52 (2015).
4. Singh, N. P., Rani, M., Gupta, K., Sagar, T. & Kaur, I. R. Changing trends in antimicrobial susceptibility pattern of bacterial isolates in a burn unit. *Burns* **43**, 1083–1087 (2017).
5. Yasidi, B. M. *et al.* Retrospective analysis of bacterial pathogens isolated from wound infections at a Tertiary Hospital in Nguru, Yobe State Nigeria. *Am. J. Biomed. Life Sci.* **3**, 1–6 (2015).
6. Barsoumian, A. E. *et al.* Clinical infectious outcomes associated with biofilm-related bacterial infections: a retrospective chart review. *BMC Infect. Dis.* **15**, 223 (2015).
7. Liu, Y. *et al.* Nanotechnology-based antimicrobials and delivery systems for biofilm-infection control. *Chem. Soc. Rev.* **48**, 428–446 (2019).
8. Le Ouay, B. & Stellacci, F. Antibacterial activity of silver nanoparticles: a surface science insight. *Nano Today* **10**, 339–354 (2015).
9. Panáček, A. *et al.* Strong and nonspecific synergistic antibacterial efficiency of antibiotics combined with silver nanoparticles at very low concentrations showing no cytotoxic effect. *Molecules* **21**, 26 (2016).
10. Jyoti, K., Baunthiyal, M. & Singh, A. Characterization of silver nanoparticles synthesized using Urtica dioica Linn. leaves and their synergistic effects with antibiotics. *J. Radiat. Res. Appl. Sci.* **9**, 217–227 (2016).
11. Panáček, A. *et al.* Silver nanoparticles strongly enhance and restore bactericidal activity of inactive antibiotics against multiresistant Enterobacteriaceae. *Colloids Surfaces B Biointerfaces* **142**, 392–399 (2016).
12. Morones-Ramirez, J. R., Winkler, J. A., Spina, C. S. & Collins, J. J. Silver enhances antibiotic activity against gram-negative bacteria. *Sci. Transl. Med.* **5**, 190ra81-190ra81 (2013).
13. Cotter, P. D., Hill, C. & Ross, R. P. Food microbiology: bacteriocins: developing innate immunity for food. *Nat. Rev. Microbiol.* **3**, 777 (2005).
14. de Arauz, L. J., Jozala, A. F., Mazzola, P. G. & Penna, T. C. V. Nisin biotechnological production and application: a review. *Trends Food Sci. Technol.* **20**, 146–154 (2009).
15. Shin, J. M. *et al.* Biomedical applications of nisin. *J. Appl. Microbiol.* **120**, 1449–1465 (2016).
16. Singh, G. *et al.* Green synthesis of silver nanoparticles using cell extracts of Anabaena doliolum and screening of its antibacterial and antitumor activity. *J. Microbiol. Biotechnol* **24**, 1354–1367 (2014).

17. Fei, J. *et al.* One-pot ultrafast self-assembly of autofluorescent polyphenol-based core@ shell nanostructures and their selective antibacterial applications. *ACS Nano* **8**, 8529–8536 (2014).
18. Chopra, M., Kaur, P., Bernela, M. & Thakur, R. Surfactant assisted nisin loaded chitosan-carageenan nanocapsule synthesis for controlling food pathogens. *Food Control* **37**, 158–164 (2014).
19. Qi, X. *et al.* Covalent immobilization of nisin on multi-walled carbon nanotubes: superior antimicrobial and anti-biofilm properties. *Nanoscale* **3**, 1874–1880 (2011).
20. Wu, C. *et al.* Formation, characterization and release kinetics of chitosan/γ-PGA encapsulated nisin nanoparticles. *RSC Adv.* **6**, 46686–46695 (2016).
21. Schmitt, S. *et al.* Analysis of modular bioengineered antimicrobial lanthipeptides at nanoliter scale. *Nat. Chem. Biol.* **15**, 437 (2019).
22. Li, Q., Montalban-Lopez, M. & Kuipers, O. P. Increasing the antimicrobial activity of nisin-based lantibiotics against Gram-negative pathogens. *Appl. Environ. Microbiol.* **84**, e00052-18 (2018).
23. Cochrane, S. A. *et al.* Antimicrobial lipopeptide tridecaptin A1 selectively binds to Gram-negative lipid II. *Proc. Natl. Acad. Sci.* **113**, 11561–11566 (2016).
24. Ling, L. L. *et al.* A new antibiotic kills pathogens without detectable resistance. *Nature* **517**, 455 (2015).
25. Hasper, H. E. *et al.* An alternative bactericidal mechanism of action for lantibiotic peptides that target lipid II. *Science (80-.).* **313**, 1636–1637 (2006).
26. Pettit, R. K. *et al.* Microplate Alamar blue assay for Staphylococcus epidermidis biofilm susceptibility testing. *Antimicrob. Agents Chemother.* **49**, 2612–2617 (2005).
27. Tang, H.-J. *et al.* In vitro efficacy of fosfomycin-containing regimens against methicillin-resistant Staphylococcus aureus in biofilms. *J. Antimicrob. Chemother.* **67**, 944–950 (2012).
28. Kwieciński, J., Eick, S. & Wójcik, K. Effects of tea tree (Melaleuca alternifolia) oil on Staphylococcus aureus in biofilms and stationary growth phase. *Int. J. Antimicrob. Agents* **33**, 343–347 (2009).
29. Iravani, S., Korbekandi, H., Mirmohammadi, S. V. & Zolfaghari, B. Synthesis of silver nanoparticles: chemical, physical and biological methods. *Res. Pharm. Sci.* **9**, 385 (2014).
30. Polshettiwar, V., Nadagouda, M. N. & Varma, R. S. Microwave-assisted chemistry: a rapid and sustainable route to synthesis of organics and nanomaterials. *Aust. J. Chem.* **62**, 16–26 (2009).
31. Nadagouda, M. N., Speth, T. F. & Varma, R. S. Microwave-assisted green synthesis of silver nanostructures. *Acc. Chem. Res.* **44**, 469–478 (2011).
32. Moein, M., Fooladi, A. A. I. & Hosseini, H. M. Determining the effects of green chemistry synthesized Ag-nisin nanoparticle on macrophage cells. *Microb. Pathog.* **114**, 414–419 (2018).
33. Chopra, I. The increasing use of silver-based products as antimicrobial agents: a useful development or a cause for concern? *J. Antimicrob. Chemother.* **59**, 587–590 (2007).
34. Vignoni, M. *et al.* LL37 peptide@ silver nanoparticles: combining the best of the two

worlds for skin infection control. *Nanoscale* **6**, 5725–5728 (2014).

35. Besinis, A., De Peralta, T. & Handy, R. D. Inhibition of biofilm formation and antibacterial properties of a silver nano-coating on human dentine. *Nanotoxicology* **8**, 745–754 (2014).
36. Qin, H. *et al.* In vitro and in vivo anti-biofilm effects of silver nanoparticles immobilized on titanium. *Biomaterials* **35**, 9114–9125 (2014).
37. Markowska, K., Grudniak, A. M. & Wolska, K. I. Silver nanoparticles as an alternative strategy against bacterial biofilms. *Acta Biochim. Pol.* **60**, (2013).
38. Wiegand, I., Hilpert, K. & Hancock, R. E. W. Agar and broth dilution methods to determine the minimal inhibitory concentration (MIC) of antimicrobial substances. *Nat. Protoc.* **3**, 163 (2008).
39. Zhao, X. *et al.* Antiviral properties of resveratrol against pseudorabies virus are associated with the inhibition of IκB kinase activation. *Sci. Rep.* **7**, (2017).